J Therm Anal Calorim (2010) 99:391–397
DOI 10.1007/s10973-009-0199-9

Synthesis and thermal analysis of disubstituted propiolates bearing terphenylene mesogen

**Lie Chen · Yiwang Chen · Weihua Zhou ·
Xiaohui He · Yanlin Song · Zhijie Zhang**

Received: 15 February 2009 / Accepted: 29 May 2009 / Published online: 19 June 2009

Abstract Novel disubstituted propiolates bearing chromophoric terphenylene mesogenic groups, namely, 4′-cyano-4-terphenylyl-2-octynate M(CN) and 4′-methoxyl-4-terphenylyl-2-octynate M(OCH_3) are synthesized, where the terphenyl groups are connected to the C≡C through ester linkage directly. Using transition-metal catalysts such as the classical $MoCl_5$- and WCl_6-based metathesis catalysts, the polymerization of the M(CN) and M(OCH_3) are carried out in a series of different solution, however, did not obtain any products. It suggests that the WCl_6- and $MoCl_5$-based catalysts are poisoned by the polar groups, on the other hand, the bulk terphenyl groups and the long alkyl chain around the C≡C bond might inhibit the reaction. M(CN) displays monotropic nematicity, whereas M(OCH_3) exhibits enantiotropic nematicity and smecticity (SmA_d) with a bilayer arrangement when cooled and heated. Ultraviolet spectroscopy and photoluminescence measurements also show that the terphenyl groups endow disubstituted propiolates with strong UV light absorption and high photoluminescence.

Keywords Disubstituted propiolates · Liquid crystallinity · Terphenyl

Introduction

Liquid crystalline conjugated polymers have been extensively studied for their intriguing applications and stimulate technological innovations in the development of novel electronic and photonic devices such as liquid crystal displays (LCD), light-emitting diodes (LED), photovoltaic cells, film transistors and plastic lasers [1–3]. Polyacetylene is an archetypal conjugated macromolecule and its functionalization has attracted much synthetic effort over the past decades [4–7]. Compared to the instability and intractability of polyacetylene, substituted polyacetylenes show thermal stability, good solubility, excellent luminescence and photoconductivity by introducing different mesogens [8]. Introducing the orientable mesogenic moieties onto a conjugated polymer backbone, the main chain can be aligned by virtue of spontaneous orientation of the LC side chain and macroscopic alignment of LC domains is also achieved by an external force such as shear stress, electric or magnetic field [9]. Recently, a variety of polyacetylenes containing liquid-crystalline mesogens, optical nonlinearity and light-emitting chromophores have been prepared [10–22].

Recent studies have revealed that electrical and luminescence behaviors of polyacetylenes can be greatly tuned by changing their molecular structures. Generally, the mono- and disubstituted type exert great on the properties of liquid crystalline polymers, such as polynorbornene derivatives [23]. In contrast to their monosubstituted counterparts, disubstituted polyacetylenes often enjoys such advantages as being thermal stability, better film forming, mechanically much stronger and more luminescent [24–28]. Poly(1-phenyl-1-octyne) (PPO), a highly luminescent disubstituted polyacetylene, can emit light at 460 nm with high quantum yield (0.43) [29]. If the

L. Chen · Y. Chen (✉) · W. Zhou · X. He
Institute of Polymers/Institute for Advanced Study,
Nanchang University, Xuefu Road 999, Nanchang 330031,
People's Republic of China
e-mail: ywchen@ncu.edu.cn

Y. Song · Z. Zhang
Key Laboratory of Organic Solids, Centre for Molecular
Science, Institute of Chemistry, Chinese Academy of Sciences,
Beijing 100080, China

functional pendants were directly attaching to the polyacetylene backbone, the functional groups also altered the properties of the polymers. Substituted propiolates ($RC\equiv CCO_2R$), in which the carbonyloxy group and the triple bond are located in immediate vicinity, were found that the propiolic carbonyloxy groups in the neighborhood of the main-chain double bonds electronically perturbed and sterically rigidified the polyene, which in turn altered the thermal stability, liquid crystallinity, and luminescence behaviors of the polypropiolates [30]. Conjugated polymers containing mesogenic and chromophoric units can potentially show very high carrier mobility and emit polarized light [31]. Its monosubstituted derivatives of general structure $-[CH\equiv C(Ar)]n$ or poly(1-arylacetylenes) are incapable of emitting intense light, but chromophore-containing poly(1-alkylacetylene) or poly(1-alkynes) $\{-[CH\equiv C(CmH_{2m+1}-Ch)]n$ (Ch, light-emitting chromophore$\}$ can be highly luminescent [32].

The terphenyl is not only a chromophore but also a mesogenic core [33, 34], especially for cyanoterphenyl derivatives, which have been used in the preparation of a wide range of nematic mixtures and, in general, these have high thermal stability as well as chemical and photochemical stability [35]. Incorporation of terphenyl chromophore with auxochrome tails into the electronically active polyacetylenes chains is of particular interest, because the spontaneous orientation and chromophoric property of the terphenyl mesogens might likely lead to materials with novel, outstanding and interesting properties. Thus, in order to obtain the attractive properties of liquid crystalline polyacetylenes, we designed disubstituted propiolates containing terphenyl chromophoric mesogenic groups with auxochrome tails (–CN and $-OCH_3$), where the terphenyl groups are connected to the $C\equiv C$ through ester linkage, directly (shown in Scheme 1). The photoluminescence probably could be enhanced by its constitutional repeat unit of $-RC=CCO_2Ar-$, which is not only conjugated, but also polarized by the intramolecular push–pull interaction. We also carried out their polymerization, but could not obtain any products due to metal-based catalysts poisoned by the polar groups. Here, we are concentrated on the effects of the structural variations on themesomorphic, light emitting behaviors and thermal properties of the disubstituted propiolates, and the influence of the structures on the polymerization has also been investigated.

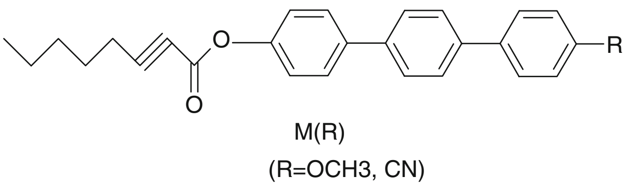

Scheme 1 The chemical structures of compounds

Experimental

Materials

n-Butyllithium, trimethyl borate, 4-(4-bromophenyl)phenol, 2-octynoic acid, tetrakis(triphenylphosphine)palladium(0), and diethyl azodicarboxylate (DEAD), 40% in toluene were purchased from Alfa Aesar and used as received without any further purification. Tetrahydrofuran (THF), toluene and dioxane were dried over sodium. Other chemicals were obtained from Shanghai Reagent Co., Ltd., and used as received.

Techniques

The nuclear magnetic resonance (NMR) spectra were collected on a Bruker ARX 400 NMR spectrometer with deuterated chloroform or THF as the solvent and with tetramethylsilane ($\delta = 0$) as the internal standard. The infrared (IR) spectra were recorded on a Shimadzu IRPrestige-21 Fourier transform infrared (FTIR) spectrophotometer by drop-casting sample solution on KBr substrates. Thermogravimetric analysis (TGA) was performed on a PerkinElmer TGA 7 for thermogravimetry at a heating rate of 20 °C/min under nitrogen with a sample size of 8–10 mg. Differential scanning calorimetry (DSC) was used to determine phase-transition temperatures on a Perkin-Elmer DSC 7 differential scanning calorimeter with a constant heating/cooling rate of 10 °C/min. Texture observations by polarizing optical microscopy (POM) were made with a Nikon E600POL polarizing optical microscope equipped with an Instec HS 400 heating and cooling stage. The X-ray diffraction (XRD) study of the samples was carried out on a Bruker D8 Focus X-ray diffractometer operating at 30 kV and 20 mA with a copper target ($\lambda = 1.54$ Å) and at a scanning rate of 1°/min.

Synthesis of disubstituted propiolates

All the reactions and manipulations were carried out under a nitrogen atmosphere.

4-Cyanobenzeneboronic acid [1(CN)]

A solution of *n*-butyllithium (30 mL, 2.87 M in hexane, 0.086 mol) was added dropwise to a stirred, cooled (−110 °C) solution of 4-bromobenzonitrile (15 g, 0.082 mol) in dry THF (180 mL) under dry nitrogen. The solution was stirred at below −100 °C for 1 h and a solution of trimethyl borate 20.8 mL in dry THF (60 mL) was added at below −100 °C. The solution was allowed to warm to room temperature overnight. 10% hydrochloric acid was added and the solution was stirred for 1 h at room temperature. The product was extracted into ether and the organic layer was washed with water and dried with $MgSO_4$. The solvent was removed in vacuo and the crude product dissolved in THF and precipitated with *n*-hexane to give a yellow solid with yield of 70%. **1**(**OCH$_3$**), white solid, the synthesis route is the same to **1**(**CN**). **1**(**R**) was used directly without further purified in the next steps.

4-Hydroxy-4′-cyanoterphenyl [2(CN)]

Under a dry nitrogen atmosphere a solution of 2.00 g of 4-cyanobenzeneboronic acid (13.6 mmol) in 10 mL of ethanol was added to a solution of 2.75 g of 4-(4-bromophenyl)phenol (97%, 11.02 mmol) and 0.42 g of tetrakis (triphenyl phosphine) palladium(0) (99%, 0.36 mmol) in 20 mL of benzene and 20 mL of aqueous Na_2CO_3 (2 M). The reaction was conducted under reflux overnight. The reaction mixture was then shaken with ethyl acetate and the insoluble parts were filtered off. The organic layer was dried with anhydrous $MgSO_4$, and the solvent was removed by evaporation in vacuo. The crude product was recrystallized from acetone to provide a yellow powder, 65% yield.

2(**CN**), IR (KBr, cm^{-1}): 2215 (C≡N), 3351 (–OH). ^{1}H-NMR (ppm, $CDCl_3$): 7.73–7.65 (four d, aromatic, 8H), 7.53 (d, aromatic, 2H ortho to cyano), 6.93 (d, aromatic, 2H ortho to hydroxyl), 4.91 (s, 1H, −OH).

2(**OCH$_3$**), colorless crystal, IR (KBr, cm^{-1}):3393, 2956, 2835, 1608, 1491, 1251, 1031, 815, 644. ^{1}H-NMR (ppm, $CDCl_3$): 7.60–7.51 (m, aromatic, 8H), 7.00–6.99 (d, aromatic, 2H ortho to hydroxyl), 6.90, 6.93 (d, aromatic, 2H ortho to OCH_3), 5.52 (s, 1H, –OH).

4′-Cyano-4-terphenylyl-2-octynate [M(CN)]

2-Octynoic acid (1.68 g, 12 mmol) was added to a mixture of 4-hydroxy-4′-cyanoterphenyl (2.71 g, 10 mmol), (dimethylamino)pyridine, DMAP 1.47 g (12 mmol), and dicyclohexylcarbodiimide, DCC (2.46 g, 12 mmol), in 30 mL of absolute THF and further stirred for 24 h at room temperature under an argon atmosphere. After the reaction finished, the solvent was removed by evaporation. The crude product was purified by column chromatography (*n*-hexane/$CHCl_3$ = 1/2) to afford M(CN) as white powder. Yield >81%.

M(CN), IR (KBr, cm^{-1}): 3037, 2930, 2861, 2222, 1727, 1605, 1483, 1385, 1111, 814. ^{1}H-NMR (ppm, $CDCl_3$): 7.75–7.60 (m, aromatic, 10H), 7.18–7.14 (d, aromatic, 2H ortho to –OOC–), 3.04–3.01 (t, 2H, $–OOC{\equiv}CCH_2$), 1.83–1.79 (m, 2H,$–CH_2CH_2C{\equiv}$), 1.46–1.29 (m, 4H, $–CH_2CH_2–$), 0.96–0.94 (t, 3H, $–CH_3$).

M(OCH_3), while powder, IR (KBr, cm^{-1}): 3037, 2928, 2852, 1725, 1611, 1483, 1379, 1110, 814. ^{1}H-NMR (ppm, $CDCl_3$): 7.71–7.51 (m, aromatic, 8H), 7.17, 7.13 (d, aromatic, 2H ortho to –OOC–), 7.00, 6.98 (d, aromatic, 2H ortho to $–OCH_3$), 3.87 (s, 3H, $–OCH_3$), 3.03–2.99 (t, 2H, $–OOC{\equiv}CCH_2$), 1.82–1.79 (m, 2H, $–CH_2CH_2C{\equiv}$), 1.46–1.25(m, 4H, $–CH_2CH_2–$), 0.95–0.92 (t, 3H, $–CH_3$).

Results and discussion

Synthesis of disubstituted propiolates

Disubstituted propiolates were synthesized by three steps: **1**(**R**) were prepared by 4-R-bromobenzene, *n*-Butyllithium and trimethyl borate, followed by the synthesis of [**2**(**R**)] through Suzuki reaction between the compounds of **1**(**R**) and 4-(4-bromophenyl) phenol using tetrakis(triphenylphosphine)palladium(0) as the catalyst. The monomers were synthesized through a esterification reaction route in the presence of 1,3-dicyclohexylcarbodimine (DCC) and 4-(dimethylamino)pyridine (DMAP). All the intermediate and final products were thoroughly purified and fully characterized, and satisfactory analysis data were obtained (detailed spectroscopic data for the key intermediates and for all the compounds being given in the Experimental section).

Structural characterization

Disubstituted propiolates were characterized by spectroscopic methods and all the products gave satisfactory data corresponding to their expected molecular structures (see Experimental section for details). In the IR spectra of M(CN) and M(OCH_3), the C=O absorption bands of the monomer M(CN) and M(OCH_3) are observed at 1,725 cm^{-1}. M(CN) showed a weak band at about 2,200 cm^{-1} associated with the C≡C stretch which is merged to the absorption band of C≡N at 2,221 cm^{-1}. The C≡C stretch of M(OCH_3) is too weak to be observed, because the C≡C is located at the middle of molecular structure, which absorbs the IR light with low efficiency. In the ^{1}H-NMR (400 MHz) spectra, the peaks of aromatic protons and aliphatic proton are located at about $\delta = 7.80$–7.00 and $\delta = 3.00$–0.90, respectively, and a peak at $\delta = 3.87$ is associated with the protons ($–OCH_3$) of M(OCH_3). Except the peaks of solvent and water remained in the spectra, no unexpected signals are observed in the spectra of the disubstituted propiolates and all the resonance peaks can be assigned to appropriate protons. The ^{1}H-NMR spectra as well as the IR analyses confirmed that the disubstituted propiolates were synthesized successfully.

Liquid crystallinity

Disubstituted propiolates are white crystals at room temperature and exhibit liquid crystallinity at elevated temperatures. The thermal transition behaviors of the disubstituted propiolates are examined by DSC and polarized optical microscopy (POM). The POM textures of disubstituted propiolates are displayed in Fig. 1. Disubstituted propiolates exhibited optical anisotropy when observed by POM, suggesting that the terphenyl mesogens endowed the compounds with thermotropic liquid-crystalline behavior. When M(CN) was heated to its melting point, a large number of anisotropic entities emerged, which did not disappeared until it enter the isotropic state. The droplet texture is associated with the mesophasic nature of a nematic phase, owning to the cyanoterphenyl mesogen generating the nematic texture [35]. Upon cooling, the isotropic melt (liquid) between the glass slides remained dark even after it was cooled to the solid state. We carefully repeated the observation several times but failed all the time, that is, mesomorphism is monotropic. Different from M(CN), M(OCH_3) possesses two different masophases. M(OCH_3) first entered the obvious SmA_d phase with fan texture, followed by the nematic phase with droplet texture. Cooling M(OCH_3) regenerated the SmA_d and nematic phase textures in sequence, demonstrating the enantiotropic nature of the phase transitions. The results were also identified on the base of the DSC curves and XRD measurements (be discussed later).

Disubstituted propiolates' curves under nitrogen were measured on a differential scanning calorimeter to give more information about the thermal transitions. DSC curve of the compounds are shown in Fig. 2 and the temperatures of the transition are taken from the maxima or minima of the curves for the samples. M(CN) entered the nematic phase at 153.5 °C with droplet texture in the second reheating cycle, associated with the g-N transition. The mesophase was stable in a temperature range over 21.1 °C before M(CN) finally entered its isotropic state at 174.6 °C. As indentified by POM, M(CN) could not form orderly arrangement, no peak observed in the first cooling cycle indicative of the monotropic nature of the nematic mesophase. The DSC curve of M(OCH_3) showed three transition peaks at 206.2, 192.2 and 163.1 °C in the first cooling cycle. The mesophase in this temperature range (206.2–192.2 °C) was identified to be nematic phase with droplet texture. Then the SmA_d with fan texture running across the backs of droplet texture, however, disappeared upon further cooling to 163.1 °C. Reheating M(OCH_3), three transition peaks slightly shifted to the higher temperatures were exhibited, which means the mesomorphism was enantiotropic.

With the aid of XRD measurements, more information concerning the molecular arrangements, modes of packing,

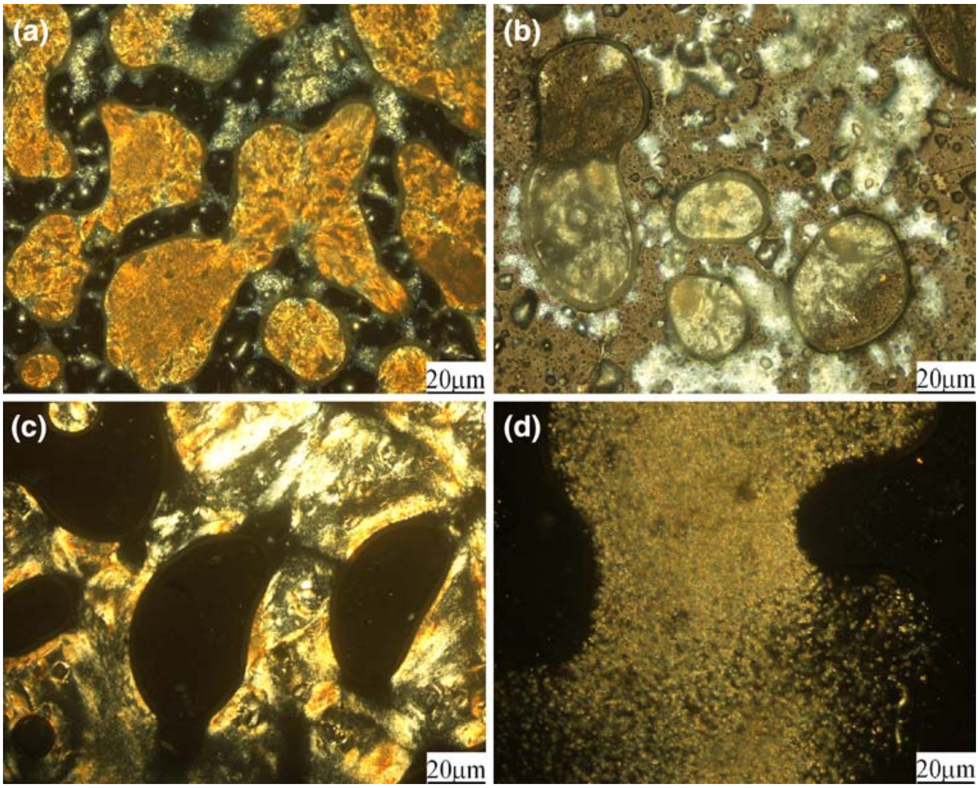

Fig. 1 Polarized optical micrographs of melts of **M(CN)** at **a** 155 °C, **b** 171 °C, and of **M(OCH_3)** at **c** 201 °C, **d** 185 °C

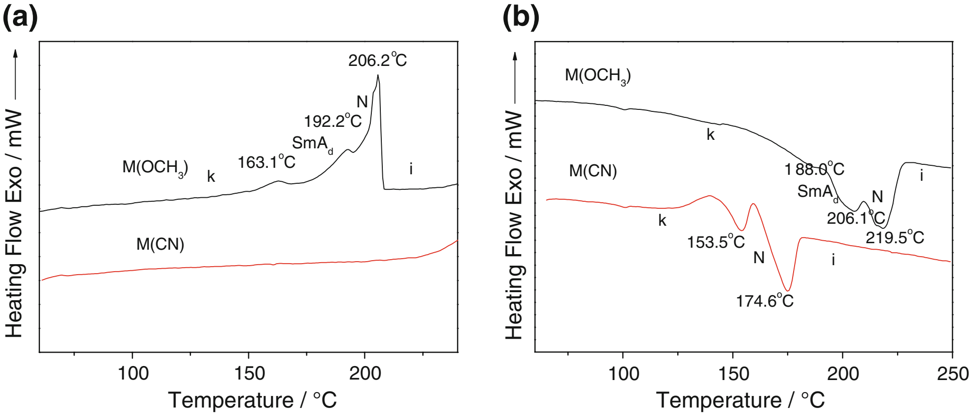

Fig. 2 DSC curves of disubstituted propiolates recorded under nitrogen during the **a** first cooling and **b** second heating scans at a scan rate of 10 K/min

and types of order in the mesophases of the acetylene liquid crystals were obtained. The XRD patterns were obtained from the mesogenic acetylene quenched with liquid nitrogen from its liquid-crystalline states, whereas the mesophases in the liquid-crystalline states at the given temperature were frozen by the rapid quenching with liquid nitrogen. The XRD diagram of M(CN) showed a broad peak in the high-angle region ($2\theta = 20.49°$), corresponding to the average intermolecular spacing of 4.33 Å (shown in Fig. 3). No reflections were observed at low angles, indicating that there is no layer ordering within the mesophases. It is known that a nematic mesophase shows only one diffuse halo at high angles. Thus, M(CN) is of nematic mesophase. However, M(OCH$_3$) showed not only the diffuse peak in the high-angle region, but also Bragg reflections at middle and low angles. The peaked at $2\theta = 19.82°$ ($d = 4.48$ Å) corresponding to the shorter preferred spacings occurring in the packing arrangement of the alkyl groups within the smectic mesophase. The sharp reflection at the low angle ($2\theta = 2.84°$) corresponds to a layer spacing of 31.23 Å, which is in considerable is excess to the molecular length in its most extended conformation (23.51 Å). This confirms the mesogens are packed in a bilayer structure. The calculated *d/l* is 1.32, a value often found in the SmA$_d$ mesophase of the liquid crystalline molecule, in which the cyanoterphenyl mesogen are interdigitated in an antiparallel fashion [36]. Interestingly, in the mid-angle region, the diffractogram of the polymer also showed a strong reflection at $2\theta = 5.1°$, from which a d-spacing of 17.21 Å was derived. The calculated length for the interdigitated {(methoxyl-terphenylyl)oxy}carbonyl groups in the proposed bilayer structure of M(OCH$_3$) is 17.06 Å. The reflection peak at $2\theta = 5.1°$ thus may be related to the regions, in which the rigid {(methoxyl-terphenylyl)oxy}carbonyl groups are interdigitated and well packed.

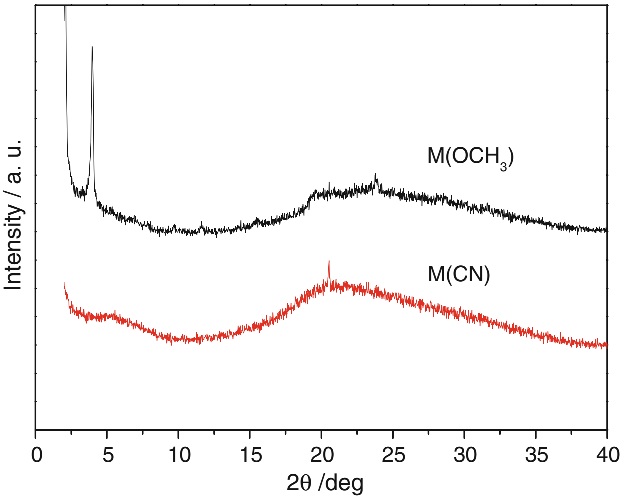

Fig. 3 X-ray diffraction patterns of disubstituted propiolates quenched from their liquid crystalline states

Electronic absorption and photoluminescent (PL)

The ultraviolet–visible (UV) and PL of M(CN) and M(OCH$_3$) in dilute CH_2Cl_2 are investigated. The incorporation of the terphenyl groups and the unit of $-C{\equiv}CCO_2-$ into the molecular structures allows better conjugation of the molecules, which endows the monomer with strong UV absorption and high photoluminescence. The UV spectrum of M(OCH$_3$) is detected as a broad strong absorption (300–340 nm), and M(CN) is red-shifted to 350 nm. The light-emitting of M(CN) is stronger and also 50 nm red-shifted at about 400 nm than in the case of M(OCH$_3$) at about 350 nm. The absorption or light-emitting is red-shifted as the electron-withdrawing character of the substituent increases [33].

Conclusions

In this work, we synthesized a group of new functional disubstituted propiolates and introduced the chromophoric terphenylene mesogenic as the pendant onto propiolates.

The thermal, mesogenic, and luminescent properties of disubstituted propiolates with terphenylene were studied and the effects of the structural variations on polymerization of disubstituted propiolates also were given special attention. Disubstituted propiolates with CN terminal substituent at terphenylene displays monotropic nematicity, whereas the one with OCH_3 terminal substituent exhibits enantiotropic nematicity and smecticity (SmA_d) with a bilayer arrangement when cooled and heated. The incorporation of the terphenylene groups and the unit of $-C\equiv CCO_2-$ into the molecular structures could allow better conjugation of the monomers, which endows disubstituted propiolates with strong UV light absorption and high photoluminescence. The disubstituted propiolates bearing the polar functional groups are seems poisonous to the common transition-metal catalysts such as Mo- and W-based catalysts and the large inherent steric hindrance of the terphenyl group will further the destruction. Thus, do our effort to find out an effective catalyst for the type of disubstituted propiolates will be the next task, although it may be daunting.

Acknowledgments Financial support for this work was provided by the National Natural Science Foundation of China (50773029), the Natural Science Foundation of Jiangxi Province (2007GZC1727 and 2008GQH0046), Jiangxi Provincial Department of Education, the Program for New Century Excellent Talents in University (NCET-06-0574), and Program for Innovative Research Team of Nanchang University, Program for Innovative Research Team in University of Jiangxi Province, and Program for Changjiang Scholars and Innovative Research Team in University (IRT0730).

References

1. Forrest SR. The path to ubiquitous and low-cost organic electronic appliances on plastic. Nature. 2004;428:911–8.
2. Heeger AJ. Semiconducting and metallic polymers: the fourth generation of polymeric materials. Angew Chem Int Ed. 2001;40: 2591–611.
3. Radhakrishnan S, Somanathan N, Narashimhaswamy T, Thelakkat M, Schmidt HW. Thermal studies on polythiophene containing mesogenic side chains. J Therm Anal Calorim. 2006;85:433–8.
4. MacDiarmid AG. Synthetic metals: a novel role for organic polymers. Angew Chem Int Ed. 2001;40:2581–90.
5. Shirakawa H. The discovery of polyacetylene film: the dawning of an era of conducting polymers. Angew Chem Int Ed. 2001;40: 2575–80.
6. Yashima E, Maeda K, Nishimura T. Detection and amplification of chirality by helical polymers. Chem Eur J. 2004;10:42–51.
7. Lam JWY, Tang BZ. Functional polyacetylenes. Acc Chem Res. 2005;38:745–54.
8. Law CCW, Lam JWY, Qin A, Dong Y, Kwok HS, Tang BZ. Synthesis, thermal stability, light emission, and fluorescent photopatterning of poly(diphenylacetylene)s carrying naphthalene pendant groups. Polymer. 2006;47:6642–51.
9. Osaka I, Goto H, Itoh K, Akagi K. Dichroic fluorescence of liquid crystalline polythiophene and polythienylenevinylene derivatives. Synth Met. 2001;119:541–2.
10. Li Z, Li QQ, Qin AJ, Dong YQ, Lam JWY, Dong YP, et al. Synthesis and characterization of a new disubstituted polyacetylene containing indolylazo moieties in side chains. J Polym Sci A. 2006;44:5672–81.
11. Chen L, Chen YW, Zha DJ, Yang Y. Synthesis and properties of polyacetylenes with directly attached bis(4-alkoxyphenyl)terephthalate mesogens as pendants. J Polym Sci A. 2006;44:2499–509.
12. Wang R, Wang WZ, Yang GZ, Liu TX, Yu JS, Jiang YD. Synthesis and characterization of highly stable blue-light-emitting hyperbranched conjugated polymers. J Polym Sci A. 2008;46:790–802.
13. Lai LM, Lam JWY, Qin A, Dong Y, Tang BZ. Synthesis, helicity, and chromism of optically active poly(phenylacetylene)s carrying different amino acid moieties and pendant terminal groups. J Phys Chem B. 2006;110:11128–38.
14. Li BS, Kang SZ, Cheuk KKL, Wan L, Ling L, Bai C, et al. Self-assembling of helical poly(phenylacetylene) carrying L-valine pendants in solution, on mica substrate, and on water surface. Langmuir. 2004;20:7598–603.
15. Yuan WZ, Mao Y, Zhao H, Sun JZ, Xu HP, Jin JK, et al. Electronic interactions and polymer effect in the functionalization and solvation of carbon nanotubes by pyrene- and ferrocene-containing poly(1-alkyne)s. Macromolecules. 2008;41:701–7.
16. Yuan WZ, Qin A, Lam JWY, Sun JZ, Dong Y, Häussler M, et al. Disubstituted polyacetylenes containing photopolymerizable vinyl groups and polar ester functionality: polymer synthesis, aggregation-enhanced emission, and fluorescent pattern formation. Macromolecules. 2007;40:3159–66.
17. Yuan WZ, Sun JZ, Dong Y, Häussler M, Yang F, Xu HP, et al. Wrapping carbon nanotubes in pyrene-containing poly(phenylacetylene) chains: solubility, stability, light emission, and surface photovoltaic properties. Macromolecules. 2006;39:8011–20.
18. Okoshi K, Sakajiri K, Kumaki J, Yashima E. Well-defined lyotropic liquid crystalline properties of rigid-rod helical polyacetylenes. Macromolecules. 2005;38:4061–4.
19. Akagi K, Guo S, Mori T, Goh M, Piao G, Kyotani M. Synthesis of helical polyacetylene in chiral nematic liquid crystals using crown ether type binaphthyl derivatives as chiral dopants. J Am Chem Soc. 2005;127:14647–54.
20. Sanda F, Kawaguchi T, Masuda T, Kobayashi N. Synthesis and properties of polyacetylenes having pendant carbazole groups. Macromolecules. 2003;36:2224–9.
21. Xing C, Lam JWY, Zhao K, Tang BZ. Synthesis and liquid crystalline properties of poly(1-alkyne)s carrying triphenylene discogens. J Polym Sci A. 2008;346:2960–74.
22. Zhou J-L, Chen X-F, Fan X-H, Chai C-P, Lu C-X, Zhao X-D, et al. Synthesis and properties of azobenzene-containing poly(1-alkyne)s with different functional pendant groups. J Polym Sci A. 2006;44:4532–45.
23. Danch A, Lohner K, Ungerank M, Stelzer F. Thermal analysis of the conformational disorder in side-chain liquid crystal (SCLC) polymers with rigid backbone. Glass transition studies. J Therm Anal Cal. 1998;54:161–70.
24. Lam JWY, Tang BZ. Liquid-crystalline and light-emitting polyacetylenes. J Polym Sci A. 2003;41:2607–9.
25. Lam JWY, Dong Y, Law CCW, Dong Y, Cheuk KKL, Lai LM, et al. Functional disubstituted polyacetylenes and soluble cross-linked polyenes: effects of pendant groups or side chains on liquid crystallinity and light emission of poly(1-phenyl-1-undecyne)s. Macromolecules. 2005;38:3290–300.
26. Hua J, Lam JWY, Yu X, Wu L, Kwok HS, Wong KS, et al. Synthesis, light emission, and photovoltaic properties of perylene-containing polyacetylenes. J Polym Sci A. 2008;46:2025–37.
27. Sun RG, Wang YZ, Wang DK, Zheng QB, Epstein AJ. Hole transport in substituted polydiphenylacetylene light-emitting devices: mobility improvement through carbazole moiety. Synth Met. 2000;111:403.
28. Sun RG, Masuda T, Kobayashi T. Visible electroluminescence of polyacetylene derivatives. Synth Met. 1997;91:301–3.

29. Mi Y, Tang BZ. Advancing macromolecular science and developing functional polymeric materials. Polym News. 2001;26: 170–6.
30. Lam JWY, Luo J, Dong Y, Cheuk KKL, Tang BZ. Functional polyacetylenes: synthesis, thermal stability, liquid crystallinity, and light emission of polypropiolates. Macromolecules. 2002;35: 8288–99.
31. O'Neill M, Kelly SM. Liquid crystals for charge transport, luminescence, and photonics. Adv Mater. 2003;15:1135–46.
32. Huang YM, Ge W, Lam JWY, Cheuk KKL, Tang BZ. Electrically tunable photoluminescence of liquid crystalline polyacetylene solutions. Mater Sci Eng B. 2001;85:122–5.
33. Goulding M, Greenfield S, Parri O, Coates D. Liquid crystals with a thiomethyl end group: lateral fluoro substituted 4-(trans-4-(*n*-propyl)cyclohexylethyl)-4′-thiomethylbiphenyls and 4-*n*-alkyl-4″-thiomethylterphenyls. Mol Cryst Liq Cryst. 1995;265: 2593–606.
34. Gray GW, Harrison KJ, Nash JA. Wide range nematic mixtures incorporating 4″-*n*-alkyl-4-cyano-*p*-terphenyls. J Chem Soc Chem Commun. 1974;11:431–2.
35. Oriol L, Pinol M, Serrano JL, Martinez C, Alcala R, Cases R, et al. Synthesis and characterization of reactive liquid crystals and polymers based on terphenyl derivatives. Polymer. 2001;42: 2737–44.
36. Barny L, Dubois J-C, Friedrich C, Noel C. Polymers with terminally cyanobiphenyl-substituted side chains. A re-entrant polymorphism NSANRe. Polym Bull. 1986;15:341–8.